

Description of near- and far-field light emitted from a metal-coated tapered fiber tip

Tomasz J. Antosiewicz, Tomasz Szoplik

Faculty of Physics, Warsaw University, Pasteura 7, 02-093 Warszawa, Poland
tantos@igf.fuw.edu.pl

Abstract: We present an analytical calculation of near- and far-field radiation emitted from a metal-coated tapered fiber probe. From FDTD simulations made in Cartesian coordinates we find that charge distribution on a tip is rim localized and its density is a bipolar periodic and continuous function. Similar angular charge density distributions may result from random irregularities of tip surfaces created in the fabrication process. Thus forward emission from a tip can be described as emission of quasi-dipoles and multi-quasi-dipoles. Analytically calculated characteristics are in agreement with our FDTD simulations and previous measurements of Obermüller and Karrai.

©2007 Optical Society of America

OCIS codes: (180.0180) Microscopy; (180.5810) Scanning microscopy.

References and Links

1. H. A. Bethe, "Theory of diffraction by small holes," *Phys. Rev.* **66**, 163–182 (1944).
2. C. J. Bouwkamp, "On Bethe's theory of diffraction by small holes," *Philips Res. Rep.* **5**, 321–332 (1950).
3. Y. Leviatan, "Study of near-zone fields of a small aperture," *J. Appl. Phys.* **60**, 1577–1583 (1986).
4. D. W. Pohl, W. Denk, and M. Lanz, "Optical stethoscopy: Image recording with resolution $\lambda/20$," *Appl. Phys. Lett.* **44**, 651–653 (1984).
5. E. Betzig and J. K. Trautman, "Near-field optics: microscopy, spectroscopy, and surface modification beyond the diffraction limit," *Science* **257**, 189–95 (1992).
6. T. W. Ebbesen, H. J. Lezec, H. F. Ghaemi, T. Thio, and P. A. Wolff, "Extraordinary optical transmission through sub-wavelength hole arrays," *Nature (London)* **391**, 667–669 (1998).
7. D. E. Grupp, H. J. Lezec, T. W. Ebbesen, K. M. Pellerin, and T. Thio, "Crucial role of metal surface in enhanced transmission through subwavelength apertures," *Appl. Phys. Lett.* **77**, 1569–1571 (2000).
8. H. J. Lezec, A. Degiron, E. Devaux, R. A. Linke, L. Martin-Moreno, F. J. Garcia-Vidal and T. W. Ebbesen, "Beaming light from a subwavelength aperture," *Science* **297**, 820 (2002).
9. L. Martín-Moreno, F. J. García-Vidal, H. J. Lezec, A. Degiron, and T. W. Ebbesen, "Theory of highly directional emission from a single subwavelength aperture surrounded by surface corrugations," *Phys. Rev. Lett.* **90**, 167401 (2003).
10. F. I. Baida, D. Van Labeke, and B. Guizal, "Enhanced confined light transmission by single subwavelength apertures in metallic films," *Appl. Opt.* **42**, 6811–6815 (2003).
11. S. Astilean, P. Lalanne, and M. Palamaru, "Light transmission through metallic channels much smaller than the wavelength," *Opt. Commun.* **175**, 265–273 (2000).
12. F. Garcia de Abajo, "Light transmission through a single cylindrical hole in a metallic film," *Opt. Express* **10**, 1475–1484 (2002).
13. K. Y. Kim, Y. K. Cho, H. S. Tae and J. H. Lee, "Optical guided dispersions and subwavelength transmissions in dispersive plasmonic circular holes," *Opto-Electron. Rev.* **14**, 233–241 (2006).
14. M. I. Stockman, "Nanofocusing of optical energy in tapered plasmonic waveguides," *Phys. Rev. Lett.* **93**, 137404-1-4 (2004).
15. N. A. Janunts, K. S. Baghdasaryan, K. V. Nerkararyan and B. Hecht, "Excitation and superfocusing of surface plasmon polaritons on a silver-coated optical fiber tip," *Opt. Commun.* **253**, 118–124 (2005).
16. E. X. Jin and X. Xu, "Obtaining super resolution light spot using surface plasmon assisted sharp ridge nanoaperture," *Appl. Phys. Lett.* **86**, 111106 (2005).
17. K. Tanaka, M. Tanaka, and T. Sugiyama, "Creation of strongly localized and strongly enhanced optical near-field on metallic probe-tip with surface plasmon polaritons," *Opt. Express* **14**, 832–846 (2006).
18. H. F. Arnoldus and J. T. Foley, "Spatial separation of the traveling and evanescent parts of dipole radiation," *Opt. Lett.* **28**, 1299–1301 (2003).
19. H. F. Arnoldus and J. T. Foley, "Highly directed transmission of multipole radiation by an interface," *Opt. Commun.* **246**, 45–56 (2005).
20. D. J. Shin, A. Chavez-Pirson, Y. H. Lee, "Multipole analysis of the radiation from near-field optical probes," *Opt. Lett.* **25**, 171–173 (2000).

21. A. Drezet, J. C. Woehl, and S. Huan, "Far-field emission of a tapered optical fibre tip: a theoretical analysis," *J. Microsc.* **202**, 359-361 (2001).
 22. A. Drezet, J. C. Woehl, and S. Huan, "Diffraction by a small aperture in conical geometry: Application to metal-coated tips used in near-field optical microscopy," *Phys. Rev. E* **65**, 046611 (2002).
 23. A. Drezet, S. Huan, and J. C. Woehl, "In situ characterization of optical tips using single fluorescent nanobeads," *J. Lumin.* **107**, 176-181 (2004).
 24. C. Durkan and I. V. Shvets, "Polarization effects in reflection-mode scanning near-field optical microscopy," *J. Appl. Phys.* **83**, 1837-1843 (1998).
 25. A. Gademann, I. V. Shvets, and C. Durkan, "Study of polarization-dependant energy coupling between near-field optical probe and mesoscopic metal structure," *J. Appl. Phys.* **95**, 3988-3993 (2004).
 26. C. Obermüller and K. Karrai, "Far field characterization of diffracting circular aperture," *Appl. Phys. Lett.* **67**, 3408-3410 (1995).
 27. J. H. Kim and K. B. Song, "Recent progress of nano-technology with NSOM," *Micron* **38**, 409-426 (2007).
 28. T. Szoplik, W. M. Saj, J. Pniewski, and T. J. Antosiewicz, "Transmission of radially polarized light beams through nanoholes," Abstracts of the EOS Topical Meeting on Nanophotonics, Metamaterials and Optical Microcavities, 16-19 October 2006, Paris, France.
 29. J. D. Jackson, *Classical Electrodynamics* 3rd Ed., (John Wiley & Sons, Inc., New York 1998).
 30. O. D. Jefimenko, *Electricity and Magnetism*, (Appleton-Century-Crofts, New York 1966).
 31. K. T. McDonald, "The relation between expressions for time-dependent electromagnetic fields given by Jefimenko and by Panofsky and Phillips," *Am. J. Phys.* **65**, 1074 (1997).
-

1. Introduction

According to early works of Bethe [1] and Bouwkamp [2] it is known that light diffracted on a sub-wavelength pinhole in a perfectly conducting thin plane screen radiates into the near-field with intensity proportional to $(a/\lambda)^4$, where a is the hole diameter. This formula was then recalculated for a circular hole of a diameter 10 times smaller than the illuminating wavelength under the assumption of quasi-static surface magnetic currents and quasi-static surface electric charges distributed in the pinhole plane [3]. It was shown, that at distances bigger than $\lambda/2$ radiation of a small aperture can be approximated with exact dipole fields. When the distance from a small aperture to an illuminated object is a few times smaller than the pinhole diameter, an object may deform the aperture radiation field [3]. Control of object dependent effects is virtually impossible.

The above mentioned problem in basic research has revived when important applications in scanning near-field optical microscopy (SNOM) and near-field optics initiated by seminal papers by Pohl *et al.* [4], Betzig and Trautman [5] and Ebbesen *et al.* had appeared [6]. Idealized diffraction conditions accepted in [1-3] could not be transferred to the description of practical problems such as subwavelength apertures in metal plates surrounded by surface corrugations [*e.g.* 7-10], subwavelength cylindrical metallic channels [*e.g.* 11-13], or metal coated tapered optical fiber tips [*e.g.* 14-17]. In the last few years several theoretical and experimental papers discussed the role of traveling and evanescent waves in dipole and multipole radiation from metal coated tapered fiber tips [18-25].

Durkan and Shvets [24] and Gademann *et al.* [25] reported on an enhancement of the coupling of light from a SNOM probe into mesoscopic metal structures which depends on the polarization state of light relative to the surface structures. It was reported, that the image contrast may be improved by choosing the right polarization. Durkan and Shvets [24] experimentally observed differences in the polarization state of light emitted from different tips due to random variations of tip shape and both thickness and quality of the tip metal coating.

We are interested in forward emission modes of a metal coated tapered optical fiber tip. We suggest that random nonuniformity of the tip metal coating results in induced azimuthal periodicity of charge density distribution on a tip rim which influences SNOM resolution. We calculate the near- and far-field radiation from rim located charge distributions considered as quasi-dipoles and multi-quasi-dipoles. The calculated far-field plot is in agreement with the result of Obermüller and Karrai [26], where a local on-axis minimum in transmitted intensity plot was observed. Such a local minimum was never predicted in previously presented theoretical models.

In a recent review paper Kim and Song [27] stated that the most important challenge in SNOM development is the improvement of light throughput and strong localization of the near-field at the tip apex.

2. System and calculations

In FDTD simulations of light transmission through a nanohole in a metal screen we found that linearly, circularly and radially polarized beams induce charges with azimuthal periodicity on the aperture rim [28]. That periodicity might result from numerical solving of a cylindrical symmetry problem in the Cartesian coordinates. In practice the periodicity results from fabrication non-uniformity of the metal coating of a tip. Similar angular periodicity of rim charge density assumed by Drezet *et al.* [23] had led to quantitative confirmation of experimentally measured intensity distributions in the near-field of a tip. Here we accept simplified assumptions, 1° that the charge is located solely on a rim, and 2° the rim located charge distributions form quasi-dipoles and multi-quasi-dipoles. The multi-quasi-dipoles appear when the radial symmetry of the aperture is broken. These rim charge density distributions can be described by cosine function, with azimuthal dependence, which does not fulfill boundary conditions

$$\rho(r, \phi) \propto \cos(N\phi) \cos(\alpha t) \delta(r - R'), \quad (1)$$

where N is the number of quasi-dipoles induced on the aperture circumference and R' is a hole radius. The rim charge density distributions of Eq. (1) are illustrated in Fig. 1. In all cases the charge density amplitudes are the same, which means that the absolute charge increases linearly with the value of N .

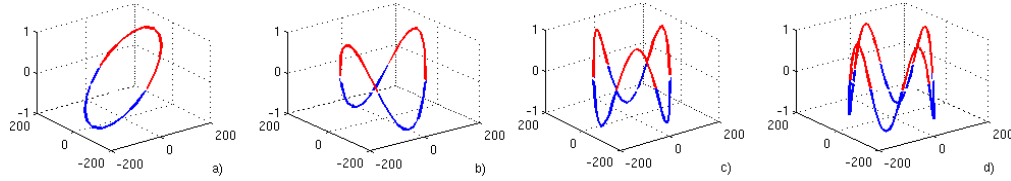


Fig. 1. Rim charge density distributions in arbitrary units for: a) $N=1$; b) $N=2$; c) $N=3$; d) $N=4$. Red indicates a value greater than zero, blue negative.

In the classical problem of an edge charge on the intersection of two conducting planes the charge distribution is expressed by a radial factor raised to a power dependent on the opening angle β between the metal planes $\rho(r) \sim r^{-n}$, where $n = \pi/\beta - 1$ [pp. 75-79 in 29]. Thus the case of a metal coated tapered probe may be described [23]

$$\rho(r, \phi) \propto \cos(N\phi) \cos(\alpha t) r^{-n}. \quad (2)$$

However, as will be proven below Eq. (1) gives a sufficient approximation to describe experimental results [26].

The current flowing on the metal rim of the aperture of a tip is calculated from the law of charge and current conservation

$$\frac{\partial}{\partial t} \rho + \vec{\nabla} \cdot \vec{J} = 0. \quad (3)$$

To calculate the desired radiation patterns in the near- and far-field we use Jefimienko's equations [Eq. (4) and (5)] [30-31], which give an explicit dependence of electric E and magnetic B fields on scalar ϕ and vectorial A potentials which are the result of charge ρ and current J distributions,

$$\vec{E}(\vec{r}, t) = \frac{1}{4\pi\epsilon_0} \times \int \left[\frac{\rho(\vec{r}', t_r)}{\mathfrak{R}^2} \hat{\mathfrak{R}} + \frac{\dot{\rho}(\vec{r}', t_r)}{c\mathfrak{R}} \hat{\mathfrak{R}} - \frac{\ddot{J}(\vec{r}', t_r)}{c^2\mathfrak{R}} \right] d\tau', \quad (4)$$

$$\vec{B}(\vec{r}, t) = \frac{\mu_0}{4\pi} \int \left[\frac{\vec{J}(\vec{r}', t_r)}{\mathfrak{R}^2} + \frac{\dot{\vec{J}}(\vec{r}', t_r)}{c\mathfrak{R}} \right] \times \hat{\mathfrak{R}} d\tau', \quad (5)$$

where \vec{r}' is a vector pointing to the radiating source, $\vec{\mathfrak{R}} = \vec{r} - \vec{r}'$, the retarded time $t_r = t - \mathfrak{R}/c$, c the speed of light in vacuum, and dot indicates a time derivative. We average the energy radiated by plasmons on the metal rim over one period to acquire energy distribution.

We use this approach instead of falling back onto known analytical solutions of radiating dipoles and multipoles because our geometry does not match the three spatial regions of interest [p. 408 in 29, 3]. In all cases the source dimensions d (the rim diameter) are in comparison to the calculation distance r a lot smaller ($d \ll r$). This is not so for the plasmon radiation approach and thus we require the above description to analyze the near-field patterns.

3. Comparison with experimental results and FDTD simulations

Radiating dipoles do not describe properly the angular characteristic of far-field radiation of SNOM tips measured by Obermüller and Karrai [26]. However, our “diluted” rim-distributed quasi-dipoles reproduce the on-axis intensity minimum (Fig. 2).

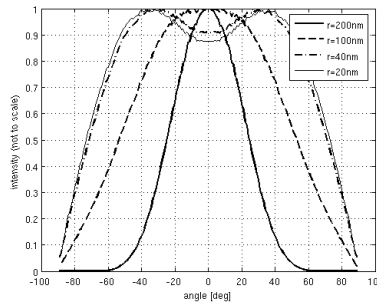


Fig. 2. Far-field angular intensities radiated by diluted dipoles of various apertures.

This is only observed for small apertures with respect to the radiating wavelength. The angular intensity minimum appears when the wavelength to aperture radius ratio $\lambda/r > 3.75$. The difference between the on-axis minimum and maximum intensity values is so small, that can not be observed in a plane perpendicular to the direction of radiation.

To confirm our assumptions we perform 3D FDTD simulations of Gaussian beam propagation in a tapered metal-coated optical fiber. The Gaussian beam’s full width at half maximum (FWHM) is chosen such that 99% of its energy couples into the fiber. We analyze field and energy distribution in various planes as well as calculate beam profiles and FWHMs.

Figure 3 shows E_x and E_y amplitudes of the electric field in the plane perpendicular to the direction of propagation at the narrow end of the tapered tip. The localization of the surface plasmon wave (high-intensity inner circle) confirms the validity of our assumption on the charge distribution on the rim of a tip. The bigger circle corresponds to the outer ridge of the metal coating.

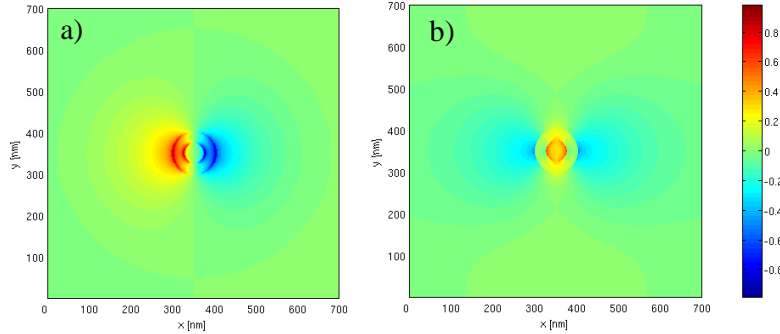


Fig. 3. Amplitude of components of the electric field (a) E_z and (b) E_y in the plane of the probe aperture. The colors indicate charges of opposite signs on the adverse sides of the aperture. The input Gaussian beam is linearly polarized along the x-axis.

The proposed model obviously cannot account for light tunneling through the metal coating. Thus side lobes in the FDTD simulated beam profiles present in Fig. 4(b) do not exist in Fig. 4(a). Moreover, the model (Fig. 4(a) black curve) neglects the non-zero value of the field within the area of the aperture that is visible in FDTD simulations (Fig. 4(b) black curve).

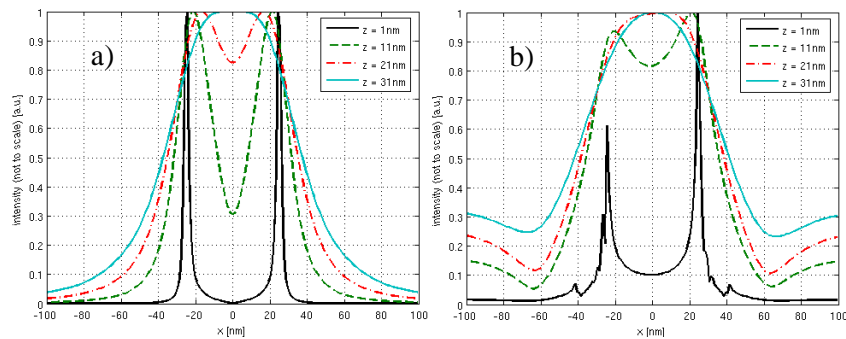


Fig. 4. Beam intensity profiles calculated at increasing distances $z = 1, 11, 21, 31$ nm from the aperture; (a) quasi-dipole model, (b) 2D FDTD simulation. Intensity curves are normalized to their respective maximum values.

Both intensity plots are directly compared in Fig. 5(a). Radiation from the aperture clearance makes the on-axis local minimum disappear at a closer distance in the FDTD simulation than in the model prediction [compare Figs. 4(a) and 4(b)]. Tunneling and aperture clearance radiation, not addressed by the quasi-dipole model, result in a broader beam observed in the FDTD simulations [Fig. 5(b)].

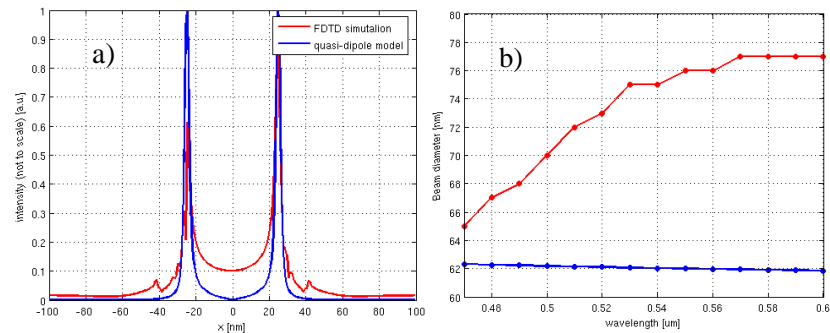


Fig. 5. (a). Field intensity in the aperture plane calculated by FDTD (red) and the multi-quasi-dipole method (blue); (b). FWHM calculated 10 nm behind the aperture using both methods, FDTD (red) and the multi-quasi-dipole method (blue).

4. Results and discussion

To analyze near-field radiation patterns for multi-quasi-dipoles we consider tapered probes with circular apertures of 20 and 40 nm radii. We scan the following parameters: beam intensity and radius as functions of wavelength, plasmon distribution and beam profiles.

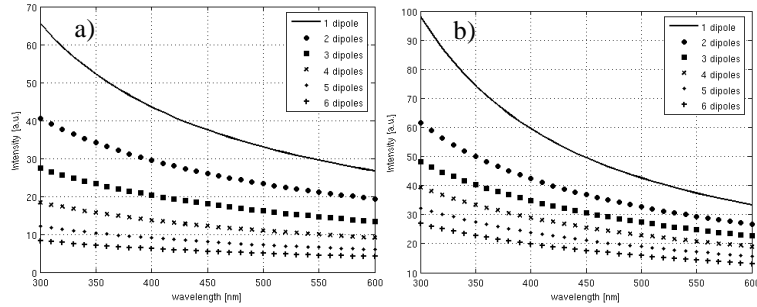


Fig. 6. Beam intensity normalized to the number of quasi-dipoles N for various multi-quasi-dipoles at a distance of 5 nm from the tips of aperture diameters a) 40 nm and b) 80 nm.

Figure 6 shows beam intensities calculated for multi-quasi-dipole radiating sources normalized to the number of quasi-dipoles N . We recall that the intensity plots are calculated for particular rim charge density distributions shown in Fig. 1 with the absolute charge proportional to N and that the polarization of the input beam is not taken into account. For both aperture diameters the intensities drop-off with increasing wavelengths. The most important radiating source is the quasi-dipole, because it is a simple approximation that describes measured SNOM radiation. We observe that this radiation intensity is comparable in intensity to radiation coming from higher order multi-quasi-dipoles. This can lead, in the presence of manufacturing inaccuracies, to a strong, unwanted signal which does not bear any resemblance to the linearly polarized light coming from a perfect SNOM tip [20, 24].

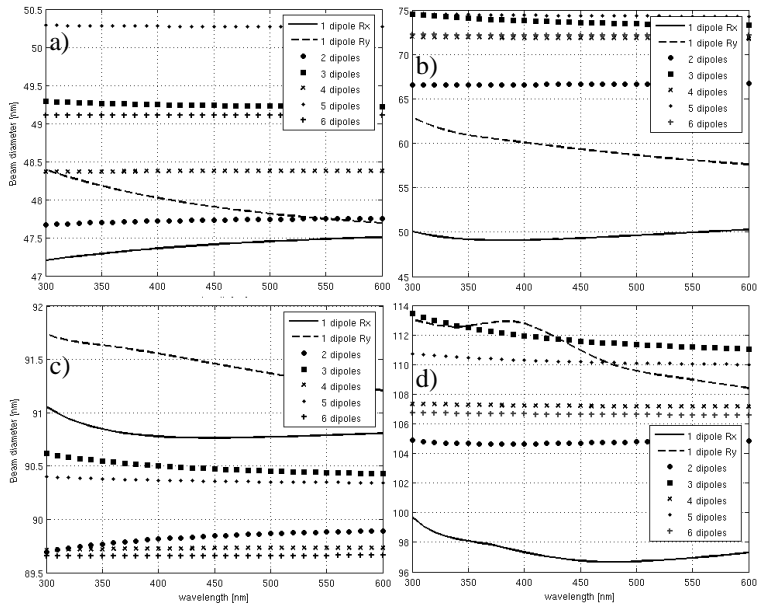


Fig. 7. Beam widths calculated within 1 nm accuracy for 40 nm (a), (b) and 80 nm (c), (d) apertures at a distance of 5 nm (a), (c) and 25 nm (b), (d) from the aperture.

Figure 7 shows FWHMs of beams radiated from 40 and 80 nm aperture diameters calculated 5 and 25 nm behind the tips. It can be seen, as noted earlier [e.g. 24, 26], that the beam diameter

and thus SNOM resolution do not depend on the wavelength used, but on the rim aperture and the distance between sample and tip. It is true for all considered radiating sources and, with the tip-sample distance being small, there is no decrease of the resolution due to the presence of higher order multi-quasi-dipoles. However, when the tip-sample distance increases above the usual working distance in shear-force microscopy, the beams radiated from higher multi-quasi-dipoles become wider. This leads to a worse resolution and can be a problem especially for larger apertures for which higher order multi-quasi-dipole radiation is stronger and diminishes more slowly than for small apertures.

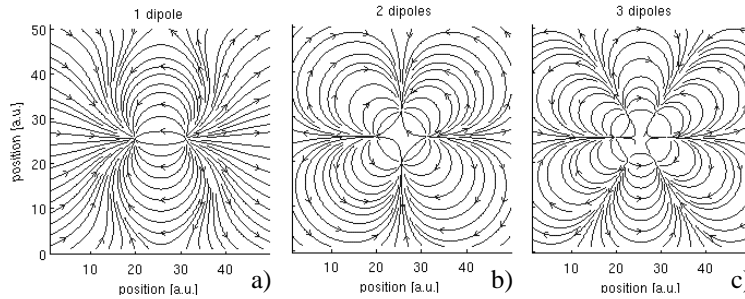


Fig. 8. Polarization of the electric field for wavelength $\lambda = 500$ nm at a distance of 25 nm from the radiating plane for an arbitrary time frame for (a) 1 quasi-dipole, (b) 2 quasi-dipoles, (c) 3 quasi-dipoles.

A single quasi-dipole radiates a beam that is almost linearly polarized [Fig. 8(a)]. However, higher order multi-quasi-dipoles emit beams with complex polarization patterns of $2\pi/N$ rotational symmetry [Figs. 8(b) and 8(c)], with N being the number of quasi-dipoles. These beams, when present and of high intensity, make it impossible to observe polarization dependant features of a sample. Then, due to the lack of linearity, the use of polarization dependant imaging enhancement reported in [24, 25] can not be achieved.

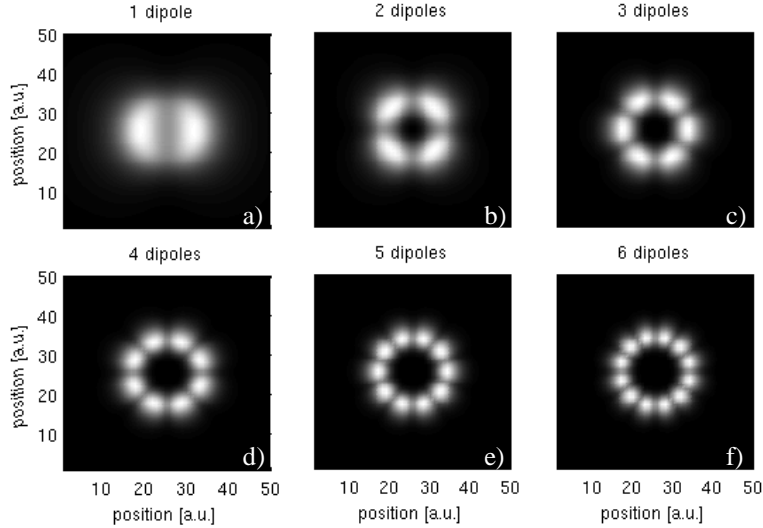


Fig. 9. Beam profiles calculated for wavelength $\lambda = 500$ nm at a distance of 25 nm from the radiating plane for (a) 1 dipole, (b) 2 quasi-dipoles, (c) 3 quasi-dipoles, (d) 4 quasi-dipoles, (e) 5 quasi-dipoles, (f) 6 quasi-dipoles (not in intensity scale).

In Fig. 9 we show the intensity patterns for six multi-quasi-dipoles at a distance of 25 nm. The single quasi-dipole produces a Gaussian profile with an on-axis minimum as expected.

5. Conclusions

We have proposed a model describing the radiating properties of metal coated tapered fiber SNOM probe. Its predictions are consistent with far-field measurements where a local on-axis minimum is observed in the angular intensity plot. This intensity minimum appears when the wavelength to aperture radius ratio λ/r exceeds a limit value $\lambda/r = 3.75$. In the accepted model the charge distributed on a metal rim of a tip forms a quasi-dipole and multi-quasi-dipoles. The quasi-dipole is induced by linearly polarized light. The latter are due to fabrication inaccuracies. At small working distances the presence of multi-quasi-dipoles does not reduce resolution. Radiation of multi-quasi-dipoles is not linearly polarized what hinders polarization assisted resolution enhancement.

We admit that the proposed model does not take into account tunneling of light through the metal coating and aperture clearance radiation. Therefore, the presented results underestimate the width of beams and thus achievable resolution.

Acknowledgments

This research was sponsored by Polish grants 3 T08A 081 27 and 37/COS/2006/03. We also acknowledge the support from the 6FP Network of Excellence Metamorphose, EC Contract #500 252.